Vibrational Nonequilibrium Modeling Framework for High-Speed Combustion Applications

Stephen Voelkel and Mark Short
Los Alamos National Laboratory
Los Alamos, New Mexico, USA

1 Introduction

Capturing the effects of vibrational nonequilibrium in high-speed flows is a challenging modeling problem. Large relaxation timescales modify reaction timescales and thermodynamic properties throughout the induction and reaction zones [1,2]. For unsteady flows, open questions remain regarding vibrational nonequilibrium in steady flow limits, regular and irregular stability limits for cellular structure, as well as the role of failure limits. This work seeks to address these questions by establishing a robust and defensible framework for modeling vibrational nonequilibrium in high-speed combustion applications. To this end, we present a new formulation focused on highlighting the important physics of nonequilibrium flows, as well as easy extension to a wide range of systems, including idealized models not directly related to any particular molecular system.

2 Vibrational Nonequilibrium Formation

For a gaseous species in thermal nonequilibrium, a single temperature description of the species' internal energy is undefined. For temperatures between 300 and 5 000 K, a vibrationally-partitioned, multi-temperature description is well-suited to describe the internal energy [1], resulting in

$$p_i = \rho_i R_i T_{tr} \quad e_i = e_{tr,i}(T_{tr}) + e_{v,i}, \tag{1}$$

where p_i is the species pressure, ρ_i is the mass density, R_i is the gas constant, T_{tr} is the translational-rotational temperature (shared by all species), and e_i is the specific internal energy with components $e_{tr,i}$ (translational-rotational) and $e_{v,i}$ (vibrational). Here, we assume $e_{tr,i} = R_i T_{tr}(3+N_{r,i})/2 + e_{o,i}$, where $e_{o,i}$ is the reference energy state and $N_{r,i}$ is the number of rotational degrees of freedom. We assume that the vibrational energy is connected to a vibrational temperature, $T_{v,i}$, via a harmonic oscillator model. The mixture equation of state is defined with Dalton's partial pressure model, given by

$$p = \rho T_{tr} \sum_{i=1}^{N} Y_i R_i, \quad e = \frac{p}{(\gamma_{tr}-1)\rho} + \sum_{i=1}^{N} Y_i (e_{v,i} + e_{o,i}), \tag{2}$$

Correspondence to: svoelkel@lanl.gov

where p, ρ, and e are the mixture pressure, density, and internal energy, respectively, Y_i is the species mass fraction, and γ_{tr} is the ratio of specific heats associated with the translational-rotational energy of the mixture (as opposed to the full ratio of specific heats γ).

The partitioned internal energy necessitates additional transport equations for each species with a vibrational energy component. The resulting one-dimensional reactive, vibrationally-partitioned Euler equations for a mixture of N species are given by

$$\frac{\partial}{\partial t}\begin{bmatrix}\rho\\ \rho u\\ \rho E\\ \rho Y_i\\ \rho Y_i e_{v,i}\end{bmatrix}+\frac{\partial}{\partial x}\begin{bmatrix}\rho u\\ \rho u^2+p\\ u(\rho E+p)\\ \rho u Y_i\\ \rho u Y_i e_{v,i}\end{bmatrix},=\begin{bmatrix}0\\ 0\\ 0\\ W_i\dot{\omega}_i\\ S_{\text{T-V},i}+S_{\text{V-V},i}+S_{\text{C-V},i}\end{bmatrix}, \tag{3}$$

for $i=1,\ldots,N$. Here, x and t denote the spatial and temporal components of the solution vector, respectively, u is the velocity, $E=e+u^2/2$ is the total energy, W_i is the species molecular mass, and $\dot{\omega}_i$ is the species molar production rate. The source terms $S_{\text{T-V},i}$, $S_{\text{T-V},i}$, and $S_{\text{T-V},i}$ describe the vibrational energy exchange processes with translational-rotational, vibrational, and chemical energy, respectively.

Chemical rates are calculated for J irreversible reactions of the form $\sum_{i=1}^{N}\nu'_{ij}\chi_i \rightarrow \sum_{i=1}^{N}\nu''_{ij}\chi_i$, where ν'_{ij} and ν''_{ij} are the species forward and reverse stoichiometric coefficients, respectively, and χ_i denotes the species (e.g. H_2), and are given by

$$\dot{\omega}_i=\sum_{j=1}^{J}\left[\left(\nu''_{ij}-\nu'_{ij}\right)\cdot\mathcal{K}_j(T_{tr},\boldsymbol{T_v})\cdot\prod_{i=1}^{N}\left(\frac{\rho Y_i}{W_i}\right)^{\nu'_{ij}}\right], \tag{4}$$

where $\mathcal{K}_j$ is the vibrationally-aware, state-averaged reaction rate. Here, we propose a generalized nonequilibrium rate form based on previous analysis and general theory [1, 3, 4], given by

$$\mathcal{K}_j(T_{tr},\boldsymbol{T_v})=\mathcal{K}_j^{eq}(T_{tr})\cdot\prod_{i=1}^{N}\varphi_{ij}(T_{tr},T_{v,i}),\quad \varphi_{ij}(T_{tr},T_{v,i})=\frac{Q_{v,i}(T_{\delta,ij})\cdot Q_{v,i}(T_{tr})^{\nu'_{ij}}}{Q_{v,i}(T^{eq}_{\delta,ij})\cdot Q_{v,i}(T_{v,i})^{\nu'_{ij}}}, \tag{5}$$

where $\mathcal{K}_j^{eq}(T_{tr})$ is the reaction rate assuming thermal equilibrium, and φ_{ij} is referred to as the vibrational efficiency function. This function enhances or inhibits reaction depending on the local vibrational temperature relative to the translational-rotational temperature and is defined as a combination of vibrational partition functions, $Q_{v,i}$, evaluated at various temperatures. Under this formulation, $T_{\delta,ij}=T_{v,i}/[\nu''_{ij}T_{v,i}/T_{tr}+\nu'_{ij}\left(1-\alpha_{v,ij}T_{v,i}/T_{tr}\right)]$ and $T^{eq}_{\delta,ij}=T_{tr}/[\nu''_{ij}+\nu'_{ij}\left(1-\alpha_{v,ij}\right)]$, where $\alpha_{v,ij}$ is the vibrational efficiency parameter.

Chemical-vibrational (C-V) energy exchange is determined by summing over the state-specific rate [3]. Subsequently, for this formulation, the exchange rate is given by

$$S_{\text{C-V},i}=W_i\sum_{j}\left[e_{v,i}(T_{\delta,ij})\cdot\left(\nu''_{ij}-\nu'_{ij}\right)\cdot\mathcal{K}_j(T_{tr},\boldsymbol{T_v})\cdot\prod_{i=1}^{N}\left(\frac{\rho Y_i}{W_i}\right)^{\nu'_{ij}}\right]. \tag{6}$$

Based on the definition of $T_{\delta,ij}$, this rate sends $T_{v,i}\rightarrow T_{tr}$ for products and $T_{v,i}\rightarrow 0$ for reactants. In other words, products are generated at the local equilibrium state and reactants consume the vibrational energy. Translational-vibrational (T-V) energy exchange rates for a mixture of harmonic oscillators are characterized by the Landau-Teller form, given by

$$S_{\text{T-V},i}=\rho Y_i\left(\frac{e^{tr}_{v,i}-e_{v,i}}{\tau_{\text{T-V},i}}\right)\quad\text{where}\quad\frac{1}{\tau_{\text{T-V},i}}=\sum_{k=1}^{N}\frac{X_k}{\tau_{\text{T-V},ik}}, \tag{7}$$

where $e_{v,i}^{tr} = e_{v,i}(T_{tr})$ as calculated for a harmonic oscillator, $\tau_{\text{T-V},i}$ is the species T-V relaxation timescale, X_k is the species molar mass fraction, and $\tau_{\text{T-V},ik}$ is the species pairwise relaxation timescale, which depends on the molecular properties of the colliding pair and the local state. Vibrational-vibrational (V-V) energy exchange pushes each species to share the same relative vibrational state and is derived from the collision rate and the probability of exchange, including constraints to ensure that the source term goes to zero at thermal equilibrium [3], given by

$$S_{\text{V-V},i} = \sum_{k \neq i}^{N} S_{\text{V-V},ik}, \quad S_{\text{V-V},ik} = W_i \cdot \frac{\rho Y_i Y_k (e_{v,i}^{tr} + e_{v,k}^{tr})}{2(W_i + W_k)\tau_{\text{V-V},ik}} \cdot \left(\frac{e_{v,k}}{e_{v,k}^{tr}} - \frac{e_{v,i}}{e_{v,i}^{tr}} \right), \quad \frac{1}{\tau_{\text{V-V},ik}} = \frac{P_{\text{V-V},ik}}{\tau_{c,ik}}, \tag{8}$$

where $\tau_{\text{V-V},ik}$ is the (symmetric) species pair-wise V-V relaxation timescale, $\tau_{c,ik}$ is the standard collision rate timescale, and $P_{\text{V-V},ik}$ is a newly employed (symmetric) V-V exchange factor. Here, we set $P_{\text{V-V},ik} = p_{\text{V-V},ik} \cdot 2e_{v,i}^{tr}/(e_{v,i}^{tr} + e_{v,k}^{tr})$, where $p_{\text{V-V},ik}$ is the V-V exchange probability, which is typically set as a constant between 10^{-6} and 10^{-2} depending on the system [1–3]. The inclusion of this symmetric $P_{\text{V-V},ik}$ term ensures that the equilibrium constraint is satisfied and that $\sum_i S_{\text{V-V},i}/W_i = 0$, which is not guaranteed under previous implementations. In general, we expect $P_{\text{V-V},ik}$ to be similar in magnitude to $p_{\text{V-V},ik}$, so the historical reference values are still valid.

3 Model Observations and Discussion

This section includes general observations and analysis of reaction rates and relaxation processes associated with the modeling choices in this work. The primary focus is on relating the nonequilibrium process to the reaction length scales in steady hydrogen detonations. For T-V exchange, we implement the correlation posed by Millikan and White [5]. Many other timescales are valid, including corrections for high temperatures, but this model is chosen due to its historical significance and to provide a general understanding of the approximate timescales in detonations. For V-V exchange, two key parameters must be defined that dictate the V-V relaxation timescale: the species pair-wise collision cross-section associated with the collision rate timescale, σ_{ik}, and exchange probability, $P_{\text{V-V},ik}$. Due to the complex nature of calculating σ_{ik}, we choose to set an average value of approximately 28 Å^2 for each pair. For the exchange probability, $p_{\text{V-V},ik}$ was originally set to a constant value of 10^{-2} based on analysis for high-speed re-entry flows [2, 3]. In measuring the vibrational-rotational relaxation process of N_2 and O_2 within high-speed turbulent diffusion flames [6], a value closer to 10^{-5} provided the best match between simulations and experimental measurements. These collective observations were used to motivate a change from $p_{\text{V-V},ik} = 10^{-2}$ to 10^{-4} for the numerical study by [1]. Here, we choose to set $P_{\text{V-V},ik}$ to a constant value, but varied between 10^{-2} and 10^{-4} to better understand how this parameter affects the relaxation process.

3.1 The Vibrational Efficiency Function

Fig. 1 shows the vibrational efficiency function for two chain-branching reactions in hydrogen-air detonations, comparing the proposed model to historical models, including a modified Park's model [7], the Coupled Vibration-Chemistry-Vibration (CVCV) model [3], and the Kuznetsov model [4]. For each reaction, we set $T_{tr} = 1500$ K and $\alpha_{v,ij} = 0.5$. Importantly, the CVCV and Kuznetsov model parameters were modified for this analysis to improve their accuracy. The CVCV model has a similar α parameter compared to this work's proposed model, which was reduced from the recommended value of 0.8 to 0.3 for these comparisons. The Kuznetsov model has a parameter that scales with the anharmonic frequency of the reactant, which was reduced from 0.3 to 0.008 for these comparisons. The modified Park's model

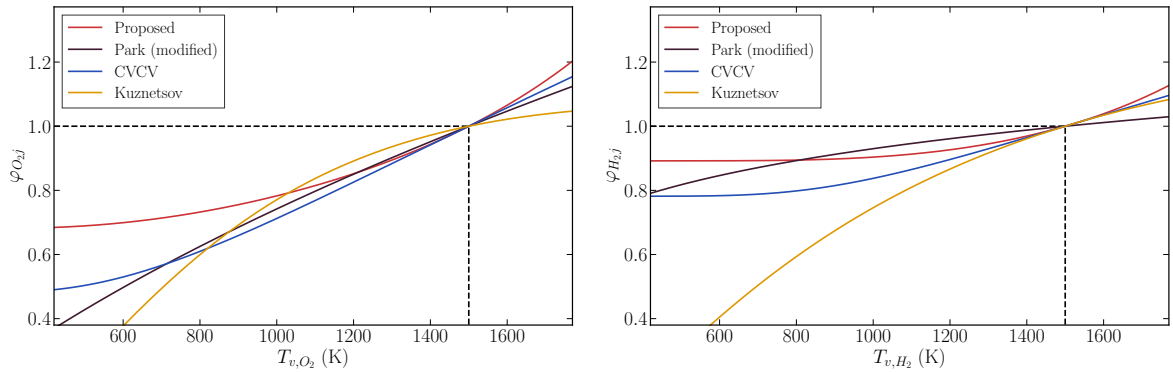

(a) $H + O_2(T_{v,O_2}) \rightarrow O + OH$ (b) $O + H_2(T_{v,H_2}) \rightarrow H + OH$

Figure 1: Vibrational efficiency function versus relative reactant vibrational temperature for key reactions in hydrogen combustion, with $T_{tr} = 1500$ K and $\alpha_{v,ij} = 0.5$.

was directly calibrated to molecular dynamics and accurate to within a few percent. Thus, this model is taken as the target for these specific reactions.

In comparing each of the models in Fig. 1, with the modified Park's model [7] representing the target, the proposed model does well. Overall, the model exhibits the same general features and efficiency values as the historical models, indicating that $\alpha_{v,ij} \approx 0.5$ is suitable for this class of reactions. Furthermore, the current model accounts for the lower characteristic vibrational temperature associated with H_2, resulting in an efficiency function closer to unity for H_2 as reactants compared to O_2, similar to the CVCV and modified Park's models. Unlike to the CVCV model, this proposed model does not require the dissociation energy associated with each molecule.

3.2 Post-Shock Vibrational Relaxation

In a VNEQ flow, T-V exchange pushes each species towards thermal equilibrium independently, whereas V-V exchange redistributes vibrational energy so that the bulk vibrational energy associated with the mixture is in balance. Overall, these two processes results in a complex vibrational relaxation process, which is illustrated by a relatively simple post-shock relaxation process as shown in Fig. 2. Here, three relaxation profiles are shown with varied $P_{\text{V-V},ik}$. The equilibrium temperature, T_{eq}, denotes the temperature corresponding to the specific internal energy as calculated from the conserved flux relations assuming thermal equilibrium.

When $P_{\text{V-V},ik} = 0$, only T-V exchange is active and each species relaxes independently. Because O_2 has a low characteristic vibrational temperature compared to H_2 and N_2, its vibrational modes are excited more rapidly and thus relaxes first. Considering that the induction and reaction zone lengths associated with the steady detonation of the same mixture assuming vibrational equilibrium are only approximately 0.02 cm and 0.6 cm, respectively, these results indicate that H_2 will exhibit significant vibrational nonequilibrium throughout the reaction zone and beyond. When $P_{\text{V-V},ik} = 10^{-4}$, we observe a balance in T-V and V-V exchange, with O_2 now exhibiting two distinct relaxation zones, the first of which is dominated by T-V exchange and the second dominated by V-V exchange. Both N_2 and H_2 relax more slowly but at a similar rate compared to O_2, with H_2 relaxation in particular dominated by V-V exchange. When $P_{\text{V-V},ik} = 10^{-2}$, which represents an extreme case but is historically relevant, V-V relaxation timescale is rapid compared to T-V exchange, pushing each species to share the same relative level vibrational nonequilibrium. In the resulting flow, each species relaxes towards thermal

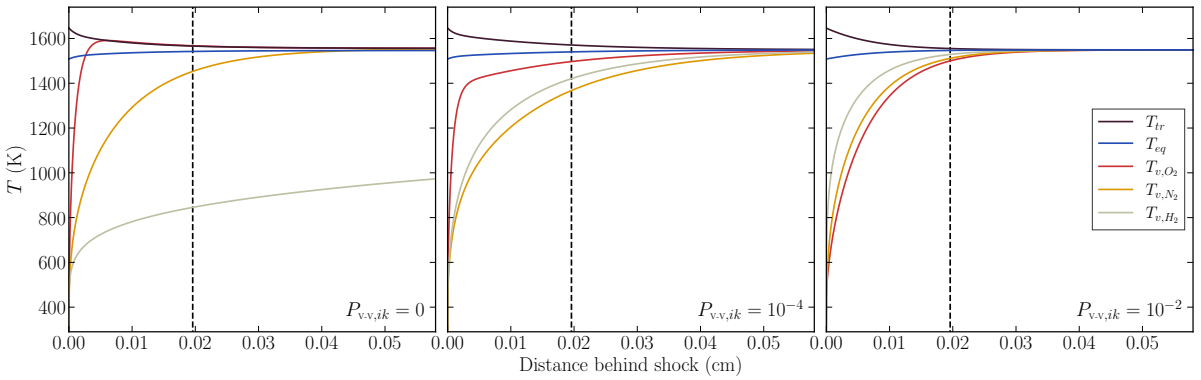

Figure 2: Post-shock temperature relaxation profiles for $2H_2 + O_2 + 3.76N_2$ propagating at $D_0 = 1980$ m/s with T-V and V-V exchange (neglecting chemical reactions). The black dashed line denotes the induction length associated with a steady detonation of the same mixture assuming vibrational equilibrium.

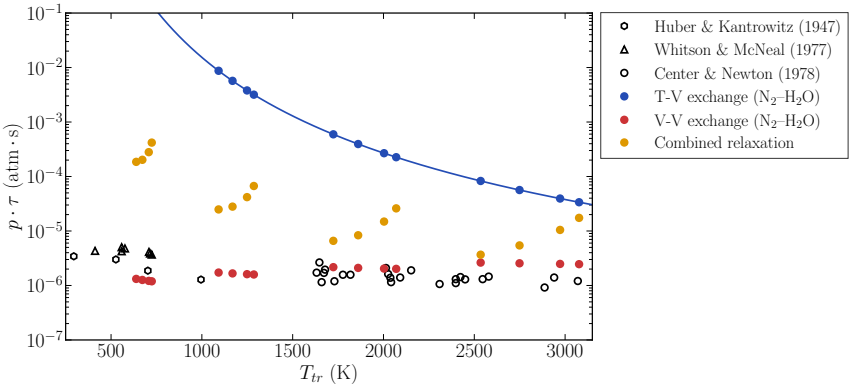

Figure 3: N_2 vibrational relaxation timescale when mixed with H_2O. The black open markers denote the experimentally measured relaxation time scale of N_2 mixed with H_2O (collated in [8]). The colored markers indicate relaxation timescales extracted from inert shock simulations at varied H_2O concentrations (between 0.1 and 1.0 moles) and wave speeds (between 1 000 and 2 500 m/s), with the blue line denoted the T-V relaxation process calculated via the analytical expression for $\tau_{\text{T-V},ik}$.

equilibrium at a similar rate, and mixture thermal equilibrium is achieved more rapidly compared to the other cases. Overall, this represents a complete shift in the relaxation dynamics, which would in turn may dramatically alter the reaction dynamics within the induction zone.

3.3 The Role of Effective Colliders

The complexity of vibrational nonequilibrium relaxation processes are amplified for more realistic applications, where other chemical and physical conditions may come into play. Of particular note is the presence of additional effective colliders, such as humidity via water vapor, which typically reduce vibrational relaxation timescales [8]. With this in mind, Fig. 3 shows the post-shock vibrational relaxation timescale of N_2 mixed with H_2O under various conditions (with $P_{\text{V-V},ik} = 10^{-4}$). The blue markers, which correspond to the extracted T-V relaxation timescale of N_2 via H_2O collisions, overlap with the line determined from the analytical expression for $\tau_{\text{T-V},ik}$, as expected. Compared to the empirical measurements, it is clear that the T-V exchange is insufficient to fully capture this relaxation process. The

red markers, which correspond to the extracted V-V relaxation timescale, are significantly lower, suggesting that V-V exchange is the dominant relaxation process. The yellow markers correspond to the combined relaxation timescale including both T-V and V-V exchange and was calculated based on the distance behind the shock wherein $T_{v,N_2} - T_{tr} \leq 5$ K divided by the wave speed. For $T_{tr} > 1500$ K (as expected in detonating flows), the combined relaxation timescale is within an order of magnitude of the experimental measurements [8]. Not only does this comparison suggest that V-V is critical for this particular relaxation process, it also supports our choice for $P_{\text{V-V},ik}$.

4 Conclusions

A generalized framework for modeling vibrational nonequilibrium in continuum-scale applications with temperatures below 5 000 K has been presented. This framework lays out how to partition the internal energy and how this modifies the transport equations. Beyond this, we presented a new modified efficiency function valid for a wide range of complex and idealized systems. The vibrational exchange terms were also presented, with the C-V exchange term formally derived for the modified efficiency function, and the V-V exchange term modified with a new, symmetric exchange probability. This model was then used to analyze coupled hydrodynamic-relaxation processes for an inert shock.

References

[1] S. Voelkel, D. Masselot, P. L. Varghese, and V. Raman, "Analysis of hydrogen-air detonation waves with vibrational nonequilibrium," in *AIP Conference Proceedings*, vol. 1786, no. 1. AIP Publishing, 2016, p. 070015.

[2] R. Fiévet, S. Voelkel, H. Koo, V. Raman, and P. L. Varghese, "Effect of thermal nonequilibrium on ignition in scramjet combustors," *Proceedings of the Combustion Institute*, vol. 36, no. 2, pp. 2901–2910, 2017.

[3] O. Knab, H.-H. Frühauf, and E. Messerschmid, "Theory and validation of the physically consistent coupled vibration-chemistry-vibration model," *Journal of Thermophysics and Heat Transfer*, vol. 9, no. 2, pp. 219–226, 1995.

[4] I. Arsentiev, B. Loukhovitski, and A. Starik, "Application of state-to-state approach in estimation of thermally nonequilibrium reaction rate constants in mode approximation," *Chemical Physics*, vol. 398, pp. 73–80, 2012.

[5] R. C. Millikan and D. R. White, "Systematics of vibrational relaxation," *The Journal of chemical physics*, vol. 39, no. 12, pp. 3209–3213, 1963.

[6] H. H. Reising, T. W. Haller, N. T. Clemens, P. L. Varghese, R. Fiévet, and V. Raman, "Spontaneous raman scattering temperature measurements and large eddy simulations of vibrational nonequilibrium in high-speed jet flames," in *32nd AIAA Aerodynamic Measurement Technology and Ground Testing Conference*, 2016, p. 3550.

[7] S. Voelkel, V. Raman, and P. L. Varghese, "Effect of thermal nonequilibrium on reactions in hydrogen combustion," *Shock Waves*, vol. 26, no. 5, pp. 539–549, 2016.

[8] R. Center and J. Newton, "Vibrational relaxation of n2 by h2o," *The Journal of Chemical Physics*, vol. 68, no. 8, pp. 3327–3333, 1978.